SEDIMENTOLOGY the journal of the International Association of Sedimentologists

Sedimentology (2010) **57,** 273–292 doi: 10.1111/j.1365-3091.2009.01112.x

Criteria for the recognition of acid-precipitated halite

ELLIOT A. JAGNIECKI[1] and KATHLEEN C. BENISON
Department of Geology, Central Michigan University, Mt. Pleasant, MI 48859, USA (E-mail: jagni1ea@gmail.com)

Associate Editor – Chris Scholz

ABSTRACT

Modern acid and neutral saline lakes in Western Australia are an excellent natural laboratory for testing how pH affects halite, and for developing criteria for distinguishing past acid saline waters from past neutral saline waters in the rock record. This study characterizes and compares physical, chemical and biological features in halite precipitated from acid (pH 1·7 to 4·2) and neutral (pH 6·8 to 7·3) saline lakes in southern Western Australia. Supplemental data include synthetic halite grown from acid and neutral saline solutions, as well as halite deposited in Permian acid lakes. Although physical processes of halite growth are not affected by pH, there are differences in the colour, accessory minerals, fluid inclusions and microfossils between acid and neutral halites. Acid lake halite commonly is yellow or orange in colour; neutral lake halites examined in this study are always snow white. Acid halites tend to contain abundant sulphate and iron oxide minerals, both as solid inclusions and as solids within fluid inclusions; neutral halites contain little, if any, sulphates and no iron oxides. Acid fluid inclusion freezing/melting behaviours include characteristics that differ from neutral fluid inclusion behaviours, such as lower eutectic temperatures, higher and wider temperature range of hydrohalite rims with a definable fuzzy border and more complex metastable phases. Acid halite contains 'hairy blobs', clusters of bacterial/archaeal/fungal remains and sulphate crystals, which are not found in halite from neutral lakes. This distinct assemblage of features characteristic of modern acid lake halites may serve as informal criteria for the recognition of past acid lake evaporites in the rock record.

Keywords 'Hairy blobs', accessory minerals, acid saline lakes, fluid inclusions, halite, Western Australia.

INTRODUCTION

Halite has proven to preserve a wealth of palaeoenvironmental data. Precipitation of halite is responsive to atmospheric conditions and water chemistry. Halite traps small amounts of parent water and air in the form of fluid inclusions, as well as preserving microfossils both as solid inclusions and within fluid inclusions (see Goldstein, 2001 and Lowenstein & Brennan, 2001 for summaries; Lowenstein *et al.*, 2001). Freezing/melting behaviours of neutral fluid inclusions in synthetic and natural halite have been well-documented and provide a method for determining past water salinities and major ions for many ancient halites (Haynes, 1985; Davis *et al.*, 1990). Homogenization temperatures of artificially nucleated vapour bubbles in fluid inclusions in halite have been used as proxies for past surface air temperatures (Roberts & Spencer, 1995; Benison & Goldstein, 1999; Losey & Benison, 2000; Bobst *et al.*, 2001; Satterfield *et al.*, 2005a,b). Even

[1]Present address: Department of Geological Sciences and Environmental Studies, Binghamton University, Binghamton, NY 13902, USA.

microorganisms have been preserved within halite fluid inclusions (Vreeland *et al.*, 2000; Mormile *et al.*, 2003; Schubert *et al.*, 2009).

There have been limited studies on recognizing acidity, or any direct measure of pH, in the sedimentary rock record. However, low pH significantly impacts the geology, chemistry and biology of modern environments (Alpers *et al.*, 2003; Benison *et al.*, 2007). Although many modern acid environments, including some volcanic crater lakes, hot springs and acid mine drainage streams, have been described, the only ancient acid saline lake environments documented are from Permian red beds and evaporites in the mid-continental United States (Benison *et al.*, 1998; Benison & Goldstein, 2001, 2002). The Permian Nippewalla Group and Opeche Shale were deposited and altered by acid waters with extremely low pHs (some less than 0). Benison & Goldstein (2002) suggested criteria for distinguishing other acid saline environments in the rock record. Diagnostic criteria described were the detection of bisulphate and high Al, Fe and/or Si in fluid inclusions in halite. Also noted as characteristics of the acid saline deposits were the association of evaporite minerals with iron oxides, 'acid' minerals such as jarosite and alunite, biomass of microbial remains and sulphate minerals ('hairy blobs'; Benison *et al.*, 2008), and the paucity of any carbonate minerals. In addition, the Permian acid halite contains solids, some trapped within fluid inclusions, that have been identified as gypsum ($CaSO_4 \cdot 2H_2O$), polyhalite [$K_2Ca_2Mg(SO_4)_4 \cdot 2H_2O$], glauberite [$Na_2Ca(SO_4)_2$] and other sulphate minerals.

The Archean Yilgarn Craton of southern Western Australia is an extensive region of acid and neutral salt lakes (Fig. 1) situated on recent red palaeosols and aeolian sediments and highly weathered Archean igneous and metamorphic rocks. A total of 62 lakes have been studied for their physical, chemical and biological processes and products (i.e. Benison *et al.*, 2007, 2008; Mormile *et al.*, 2007; Bowen *et al.*, 2008; Bowen & Benison, 2009). Approximately 40% of the lakes surveyed are extremely acidic (pH < 4, down to 1·5) and the regional groundwater is mostly acidic (pH *ca* 3·5). Lakes are shallow ($< 0{\cdot}5$ m), range in size from approximately < 1 to > 800 km^2, and are subject to flooding, evapoconcentration, desiccation and aeolian processes (Benison *et al.*, 2007). All lakes, whether acid or neutral, generally are hypersaline (up to 300‰ total dissolved solids) and are enriched in the common ions Na, Mg, Cl and SO_4. However, acid lakes and groundwaters are more geochemically complex. For example, many acid lakes have unusually high concentrations of Si (up to 3730 mg/l in lake water and up to 13300 mg/l in groundwater), Al (up to 3057 mg/l in lake water and up to 8017 mg/l in groundwater), and Fe (up to 403 mg/l in lake water and up to 459 mg/l in groundwater; Bowen & Benison, 2009). Measured ratios of S to SO_4^- show that there is a presence of unknown S-bearing species (probably bisulphate and sulphuric acid) in acid lakes. Bicarbonate is not detected in waters with a pH less than 5. In addition, some of the most acidic waters have elevated levels of some trace metals such as Cu, Zn, Co, Ni and Mo (Bowen & Benison, 2009). Groundwater chemistry is spatially heterogeneous, probably because of water–rock interactions with the various host rock lithologies. Lake water geochemistry is affected by this groundwater geochemical diversity, but also fluctuates temporally as a result of flooding and evapoconcentration (Benison *et al.*, 2007). All of the lakes, whether acid or neutral, precipitate chevron and cumulate halite from lake water and displacive halite from groundwater; acid lake waters also precipitate gypsum, hematite, kaolinite and basaluminite. Acid saline groundwaters precipitate displacive halite and gypsum crystals, as well as hematite, goethite, jarosite, alunite and kaolinite.

The goal of this study was to document any petrographic, chemical and biological characteristics unique to halite precipitated by acid waters to develop criteria for the recognition of acid saline deposits in the rock record. By focusing on halite from modern acid and neutral environments, bedded halite precipitated by the same physical processes in the same climate and general geological setting is compared and contrasted. The acid water chemistry is the main difference between these acid and neutral lakes.

Developing criteria for distinguishing acid halite using modern acid saline and neutral saline lakes provides a comparative approach for interpreting the general surface water pH range from which ancient halites formed. Comparing modern acid halite with Permian acid halite can allow for informal testing of acid characteristics. Understanding the characteristics of acid saline deposits is a tool not only for recognizing past acid saline environments on Earth, but also for those on Mars (Benison & LaClair, 2003; Kargel, 2004, Squyres *et al.*, 2004a,b; Benison, 2006; Benison & Bowen, 2006; Osterloo *et al.*, 2008). Acid saline systems are extreme environments that may form by an unusual sequence of chemical weathering

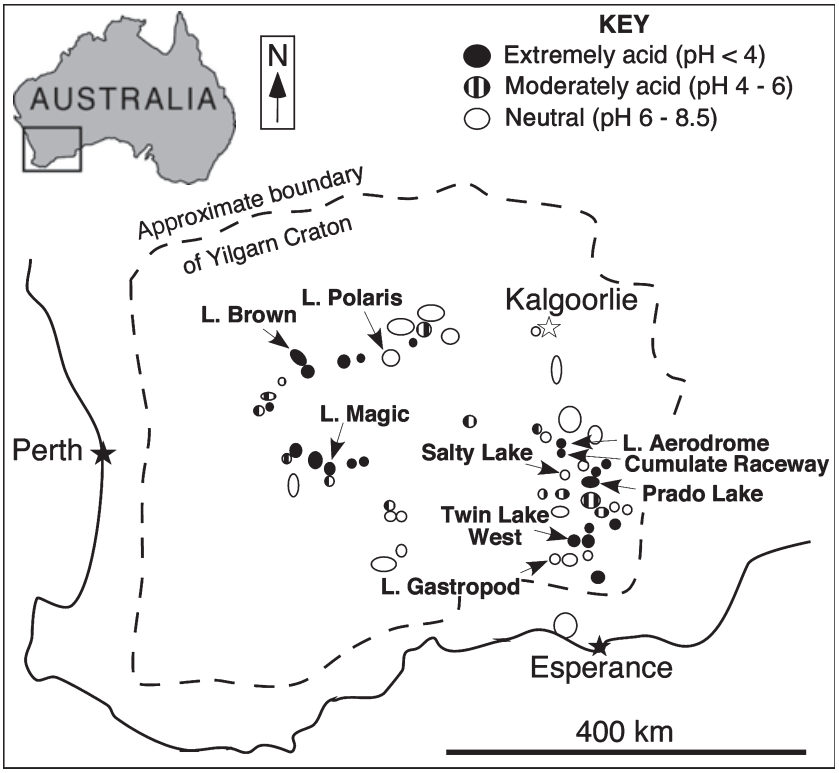

Fig. 1. Western Australia field area showing selected saline lakes on the Yilgarn Craton. Approximate locations of extremely acid and neutral lakes discussed in text are shown here. [L. = Lake]

and climate change. These systems may have implications for better understanding of mass extinctions, Precambrian sea water chemistry and the possibility of life on Mars.

APPROACH AND METHODS

The present study employed fieldwork and laboratory examinations. Halite from three acid saline lakes and three neutral saline lakes were targeted for this study. All lakes are shallow, with maximum water depths of approximately 0·5 m. The three acid lakes are Lake Magic (pH 1·7 to 2·5), Twin Lake West (pH 2·7 to 3·7) and Lake Brown (pH 3·9 to 4·8). The three neutral salt lakes are Lake Polaris (pH 7·3), Lake Gastropod (pH 6·8 to 8·5) and Salty Lake (pH 6·8 to 8·4; Fig. 1). However, other halite from acid lakes was observed in the field and sampled for laboratory comparison (Table 1).

Fieldwork was conducted in July 2001, June 2005, January 2006 and January 2008. The four field trips during different years, seasons and weather conditions allowed the temporally dynamic nature of the physical and chemical processes to be documented (Benison *et al.*, 2007). Fieldwork included observations of halite and other mineral growth, measurements of lake depth and area, and lake water and mudflat/sandflat groundwater pH, salinity and temperature. In addition, waters and sediments, including depositional halite, were sampled. The waters have been analyzed for major, minor and trace elements and compounds, and stable isotope analyses have been conducted (Bowen & Benison, 2009). Although most of the halite and water sampling was diurnal (from 06:00 to 20:00 hours), pH, salinity and temperature were measured at one lake during late nights (22:00 hours to midnight) and at three lakes during very early mornings (04:00 to 06:00 hours). Water temperatures were lower at night and in the early mornings. However, field observations showed that halite growth typically was limited to afternoons and early evenings. Therefore, the parent water temperature, pH, salinity and chemical compositions that were measured during sampling can be approximated overall for the acid and neutral halites described in this study (Table 2; Bowen & Benison, 2009).

Most halite samples were prepared for laboratory analyses by cleaving with clean razor blades to yield small halite chips (approximately 2 to 8 mm diameter, approximately 0·5 to 1 mm thick). Some halite chips were polished by hand with 800 to 1500 grade sandpaper. Representative samples of bedded halite were cut and polished with a low-speed diamond-wire saw to produce thick

Table 1 Selected field data for Western Australian lakes from which halite was collected for this study. Lake water temperatures ranged from 4 to 49 °C, depending upon season and weather. Modified after Bension *et al.*, 2007.

Saline lake	Month and year sampled	pH	Salinity (‰)	Lake stages	Chemical sediments	Major lake water chemistry	Host geology
Lake Magic	January 2006	1·7–1·9	280	Evaporation	Halite, gypsum	Cl-Na-Mg-SO_4-K-Al-Br-Si-Fe-Ca	Archean granite, recent granitic sand
Twin Lake West	July 2001	2·7	210	Evaporation	Halite, gypsum, jarosite, alunite, iron oxides, clays	Cl-Na-SO_4-Al-Mg-Ca-K	Archean gneiss, amphibolite, schist, anorthosite, quartzite, ironstone
	June 2005	3·2	200	Flooding	Halite, gypsum	Cl-Na-SO_4-Mg-K-Al-Ca-Si-Fe	
Lake Aerodrome	July 2001	2·7	130	Evaporation	Gypsum, halite, hematite, kaolinite, jarosite, alunite	Na-Cl-Mg-SO_4-Ca-Al-K-Fe	Recent quartz, gypsum, hematite sand
Prado Lake	July 2001	2·5	240	Evaporation	Halite, gypsum, jarosite, alunite, iron oxides	?	Recent quartz, gypsum, hematite, sand and sandstone
	June 2005	3·7	230	Flooding		Cl-Na-SO_4-Si-Al-Mg-Ca-K-Fe	
Cumulate Raceway	July 2001	2·7	90	Evaporation	Halite, gypsum, iron oxides	Cl-Na-$S0_4$-Mg-Ca-K-Al (during January 2006 evaporation stage)	Recent quartz, gypsum, hematite sand
Lake Brown	June 2005	4·2	215	Flooding	Halite, gypsum, jarosite, alunite, iron oxides, clays	Cl-Na-SO_4-Mg-Ca-Al-Si-K	Recent quartz, gypsum, hematite sand
	January 2006	3·9	250	Evaporation		Na-Cl-Mg-SO_4-Si-Al-Ca-K-Fe	
Lake Gastropod	January 2006	6·8	90	Flooding	Halite	Na-Cl-SO_4-Mg-Ca-K	Recent quartz sand, lignite
Salty Lake	July 2001	6·8–6·9	100	Evaporation	Halite	Cl-Na-SO_4-Mg-Ca-K	Recent quartz sand, lignite
Lake Polaris	January 2006	7·3	280	Evaporation	Halite	Cl-Na-Mg-SO_4-K-Br-Ca	Archean quartzite, recent quartz sand

sections (3 to 10 mm) for petrographic study. Contamination was not a major concern because: (i) samples were not subjected to heat, water, humidity, dust, or other fluids during preparation and storage; and (ii) most analyses focused on the halite interiors.

Various types of petrographic examination were used in this study. Optical examination was performed with transmitted, reflected and polarized light, primarily on an Olympus SZ12 low-power binocular microscope (up to 90× magnification; Olympus Optical Company Limited, Tokyo, Japan) and a Leitz Laborlux high-power microscope (up to 480× magnification; Leitz, Vila Nova de Famalico, Portugal). Photographic documentation was done with a Nikon digital camera (Nikon, Tokyo, Japan) adapted to the microscopes. Ultraviolet–visible (UV–Vis) fluorescence microscopy (using 365, 390, 400 and 450 nm wavelengths) was conducted with the use of a microscope housed in the Biology Department of Central Michigan University. Additional halite samples were

Table 2. Selected geochemical data for Western Australian lake waters from which halite was collected for this study. Major ion data given in mg/L. Data are representative of specific sites and times of halite sampling. Dashes indicate that no lake water was analyzed for this specific site and time. However, all lakes included here had water analyses performed, but for times or locations other than when halite sampling for this study was done. Modified after Bowen & Benison, 2009.

Saline lake	Month and year sampled	pH	Salinity (‰)	Na	Mg	Cl	SO_4	HCO_3	K	Ca	Br	Si	Al	Fe
Lake Magic	January 2006	1·7–1·9	280	48 000	38 400	122 000	35 200	0	4520	121	941	510	1774	331
Twin Lake West	July 2001	2·7	210	–	–	–	–	–	–	–	–	–	–	–
	June 2005	3·2	200	94 400	1890	147 000	4510	–	387	370	44	72	1903	34
Lake Aerodrome	July 2001	2·7	130	85 200	5420	75 100	4980	–	300	941	0	–	–	–
Prado Lake	July 2001	2·5	240	–	–	–	–	–	–	–	–	–	–	–
	June 2005	3·7	230	98 500	1520	150 000	3760	0	418	809	8	3730	2516	176
Cumulate Raceway	July 2001	2·7	90	–	–	–	–	–	–	–	–	–	–	–
Lake Brown	June 2005	4·2	215	85 700	1550	125 000	3380	–	289	1210	76	544	548	55
	January 2006	3·9	250	106 000	1840	67 600	1650	0	317	1330	0	2640	1815	291
Lake Gastropod	January 2006	6·8	90	–	–	–	–	–	–	–	–	28	148	28
Salty Lake	July 2001	6·8–6·9	72	–	–	–	–	–	–	–	–	–	–	–
Lake Polaris	January 2006	7·3	280	82 500	13 900	135 000	13 800	260	1170	361	384	53	194	34

analyzed with UV–Vis fluorescence microscopy at the Biological Sciences Department at Missouri University of Science and Technology and at the Kinohi Institute. Scanning electron microscopy (SEM) was conducted with a JEOL JSM-840A scanning microscope (JEOL, Tokyo, Japan).

Microthermometric analyses of fluid inclusions in halite were performed on a FLUID Inc. adapted U.S. Geological Survey gas flow heating/freezing stage (FLUID Inc, Denver, CO, USA) mounted to a Leitz Laborlux petrographic microscope. The thermocouple on the fluid inclusion stage was calibrated regularly to maintain an accuracy of ±0·1 °C over the temperature interval investigated. Freezing/melting runs on this stage involve the supercooling of the sample by liquid nitrogen until the inclusion freezes, followed by slow warming so that various phases within the inclusion can be observed at different temperatures. Multiple freezing/melting runs were conducted for each inclusion to allow for the most accurate documentation of various phases and the temperatures at which they occur, as well as to test for metastable phases (Haynes, 1985; Goldstein & Reynolds, 1994). The present study used the only available data on freezing/melting behaviour of acid inclusions, including results from synthetic halites grown from standard solutions of various pH values ($NaCl–H_2O$, $NaCl–Na_2SO_4–H_2O$ and $NaCl–Na_2SO_4–H_2SO_4–H_2O$ with pH from 0·0 to 7·0; Benison, 2002) and unpublished results from Permian acid halites. Also, observations of the freezing/melting behaviours of modern acid and neutral halites were supplemented with additional new freezing/melting data from the synthetic acid and neutral halites.

Laser Raman spectroscopy of fluid inclusions and solid inclusions in halite was conducted on a multichannel Jobin-Yvon S-3000 laser Raman microprobe (Horiba Jobin-Yvon, Kyoto, Japan) at the U.S. Geological Survey in Reston, Virginia and a Kaiser Optical System RXN1 laser Raman microprobe (Kaiser Optical Instruments Inc., Ann Arbor, MI, USA) in the Central Michigan Univer-

sity Chemistry Department. Laser Raman analyses of fluid inclusions in modern natural halite were complemented by laser Raman analyses of fluid inclusions in synthetic halites and in Permian acid halite. Because Raman spectra only represent covalently bonded compounds, the ionic nature of NaCl rules out any background noise from the host halite crystal.

Data were compared within, between and among halites from the various lakes. In particular, halites from acid lakes were compared with halites from neutral lakes. Synthetic halites, Permian acid halite, and several natural modern and ancient non-acid halites were used for comparative purposes. In addition, detailed host water geochemical data were matched with the specific lake halites to help understand the resulting physical, chemical and biological characteristics of the halites. Finally, interpretations were made about features unique to acid lake halite.

RESULTS

Halite growth

Multiple field trips over different seasons and weather conditions allowed the opportunity to make observations at both acid and neutral saline lakes during flooding, evapoconcentration and desiccation stages (Lowenstein & Hardie, 1985; Benison *et al.*, 2007). Regardless of pH, all saline lake halite grew and dissolved, in similar ways. During flooding, previously formed halite underwent at least partial dissolution, resulting in truncated crystals and formation of dissolution pipes. Halite grew rapidly during evapoconcentration. Small halite crystals grew at the air–water interface as millimetre-scale cumulate crystals. Commonly, these cumulates linked together to form 'rafts' that float on the lakes and are often pushed to the leeward lakeshore by winds. When these rafts become too heavy, they sink to the lake bottom (Shearman, 1970). At the lake bottom, halite grows upward in centimetre-scale chevron crystals (Arthurton, 1973; Shearman, 1978), forming a subaqueous crust at the lake bottom. When lakes desiccate, halite grows as a finely crystalline efflorescent halite crust by evaporation of shallow groundwaters that have wicked upward to the surface (Smoot & Lowenstein, 1991). These processes and their resulting bedded halite forms in both acid and neutral saline lakes in Western Australia have been well-observed (Benison *et al.*, 2007).

Halite colour

In the field, some colour differences in acid and neutral lakes were noted. Neutral and, at times, acid lakes contain clear water, giving the appearance of a typical freshwater lake. In contrast, some acid lakes have unusual water colours that vary through time, depending on water chemistry and concentration. For example, Lake Magic, which contains up to 1774 p.p.m. Al during evapoconcentration periods, appears bright yellow (Fig. 2) (Bowen & Benison, 2009). Unusual water colours, especially red, orange and white, in acid lakes are also formed by minerals precipitating in the lakes, such as hematite, kaolinite, basaluminite, and unidentified yellow and red hydrated sulphates and iron oxides that periodically precipitate directly from acid lake waters.

As a result of the unusual colours in acid lakes, the halite formed in acid lakes often appears to have a faint colouration. At times when halite is precipitating from yellow Lake Magic waters, the halite traps abundant yellow-water fluid inclusions. Although the solid halite is clear, the yellow fluid inclusions make the halite crystals appear yellow. Other acid lake halite is commonly pale orange, as a result of abundant hematite trapped as tiny clumps within the halite. In contrast, the halite from neutral lakes in the field area always has a snow-white colour (Fig. 2).

Most acid lakes are commonly surrounded by red, orange and/or yellow sandflats/mudflats. Acid groundwater only centimetres below the sandflat/mudflat surface rapidly precipitates early diagenetic halite, gypsum, iron oxides (mainly hematite), jarosite, alunite and kaolinite. The shallow groundwaters near the neutral lakes tend to precipitate halite and only rare gypsum. Therefore, the presence of iron oxides and jarosite at the acid lakes gives their sediment a red, orange and yellow appearance not seen at the neutral lakes.

Halite petrography

Petrographic examination of bedded halite from both acid and neutral saline lakes revealed chevron crystals and cumulate crystals (Fig. 3). Chevron crystals are centimetre-scale, upward-oriented crystals that grow at the bottom of the water body. Cumulate crystals appear as millimetre-scale, randomly oriented halite cubes that grow at the air–water interface and/or within the water column. Cumulate crystals commonly constitute a thick lamination or thin bed strati-

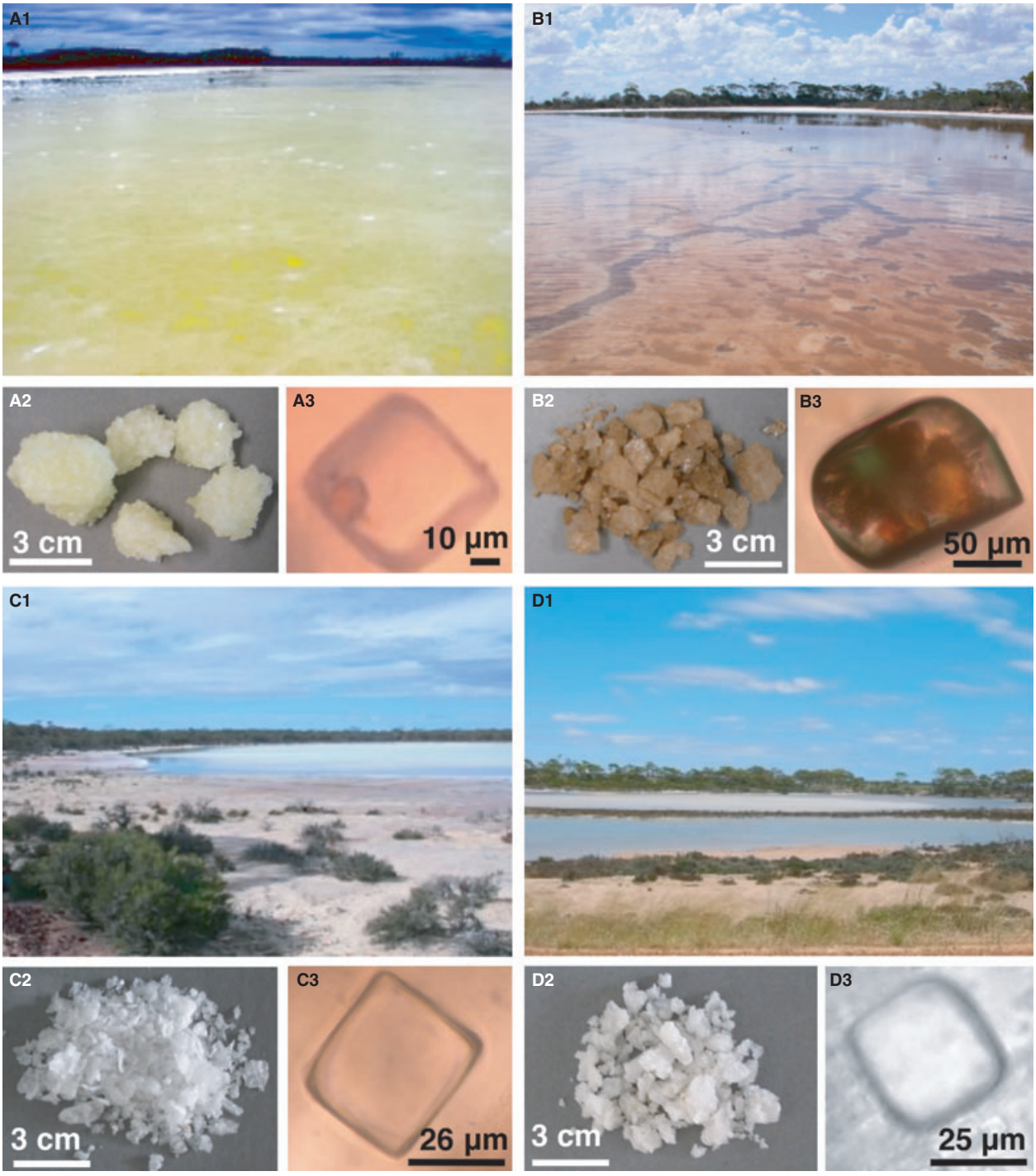

Fig. 2. Photographs showing colour variations between acid saline lakes (A) and (B) and neutral saline lakes (C) and (D). (A1) Lake Magic (at pH 1·7) contains yellow water with a high abundance of dissolved Al and actively precipitates halite and gypsum; (A2) halite is yellow with (A3) entrapped yellow solids in fluid inclusions. (B1) Lake Brown (at pH 3·9) with halite and hematite mud; (B2) halite is orange with (B3) entrapped orange, red and yellow solids in fluid inclusions. (C1) Salty Lake (pH 7·3) and (D1) Gastropod Lake (pH 6·8) both precipitate snow-white halite (C2) and (D2) with no, or extremely rare, solids within fluid inclusions.

graphically below or above chevron crystal beds. Some cumulate beds contain laterally linked cumulate crystals which probably originated as rafts.

Both chevron and cumulate halite contains abundant primary fluid inclusions, aligned in growth bands parallel to crystal faces. Many halite beds are capped by finely crystalline (sub-

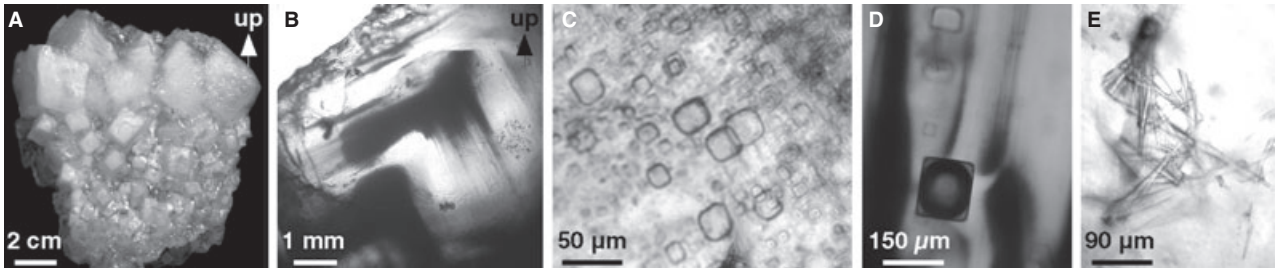

Fig. 3. Halite from acid Twin Lake West (pH 2·7 to 3·8 at times of sample collection). (A) Cross-sectional view of halite bed sampled from below 8 cm of lake water in July 2001. Smaller crystals at the bottom are cumulate crystals; larger crystals at the top are chevron crystals. (B) Thick-section of halite chevron crystal. Dark growth bands are rich in primary fluid inclusions and clear growth bands have only rare inclusions. Note the truncation of top of the chevron (probably by a flooding event), followed by successive clear halite. (C) Primary all-liquid fluid inclusions in halite. (D) Large primary fluid inclusion with liquid and a large vapour bubble (probably trapped air). (E) Gypsum needle-like crystals trapped as solid inclusions in halite.

millimetre-scale) halite interpreted as effluorescent halite crusts. Other halite beds are truncated abruptly at their tops by dissolution surfaces and are associated with vertically oriented dissolution pipes (Fig. 3B). This assemblage of sedimentary features shows that, in both acid and neutral lakes, halite growth was influenced strongly by evapoconcentration, desiccation and flooding, all processes observed in the field.

Differences in the solid inclusions in halite from the acid lakes compared with those from neutral lakes were noted. Acid lake halite contains abundant solid inclusions of gypsum (Fig. 3E) and some contain hematite inclusions. None of these types of solids were found in halite that grew in neutral saline waters (Fig. 2).

Fluid inclusion petrography

Primary fluid inclusions in both acid and neutral halite are abundant and are aligned along growth bands parallel to crystal faces. Fluid inclusions range in size from approximately 3 to 150 μm and are both square and rectangular in shape. Most fluid inclusions contain only liquid (Fig. 3C). Rare fluid inclusions contain a spherical air bubble, interpreted as atmosphere trapped as the halite grew at the water–air interface (Fig. 3D). Some fluid inclusions also contain one or more solids (Fig. 4).

Solids within fluid inclusions differ greatly between acid and neutral halite. Neutral halite contains rare solids within fluid inclusions; most of these appear to be siliceous grains from wind blown dust. The greatest diversity and abundance of solids within fluid inclusions was found in the halite from the lowest pH waters. Optical petrography indicated spherical, bladed and needle-shaped solids. Colours included clear, bright yellow, orange and red solids (Fig. 4). Some solids were birefringent and some were not.

Solids within fluid inclusions

To test whether solids within fluid inclusions were true daughter minerals (i.e. precipitated from inclusion fluid after entrapment) or were trapped accidentally (solids in the water body as the inclusion formed), representative inclusions were warmed on a heating/freezing stage. The solids did not dissolve or change shape at all, suggesting that they were trapped accidentally. In addition, the non-uniform presence (not in every inclusion) and the occurrence of similar minerals as solid inclusions within the host halite argues against them as true daughter minerals. Regardless, the presence of these minerals within the acid inclusions provides clues about the water chemistry of the acid saline lakes.

Further analyses of solids within the acid inclusions included observations under UV–Vis fluorescent light and laser Raman microscopy. Under UV–Vis fluorescence the solids do not fluoresce. Laser Raman microprobe spectroscopy shows that some solids, including bright red and some orange solids, emit high wavelength excitement, rendering them unidentifiable. However, Raman spectra of most solids show strong SO_4 peaks. The Raman spectra of synthetic hydrated sulphate minerals were compared with those of the unknown sulphate solids within fluid inclusions (Fig. 5). The synthetic standards included $CaSO_4 \cdot 2H_2O$, $MgSO_4 \cdot 7H_2O$, $FeSO_4 \cdot 4H_2O$, $ZnSO_4 \cdot 6H_2O$, $ZnSO_4 \cdot 4H_2O$ and $K_2Ca_2Mg(SO_4)_4 \cdot 2H_2O$. These data were also compared with Raman spectra of jarosite and alunite group minerals and hydrated sulphate minerals in the

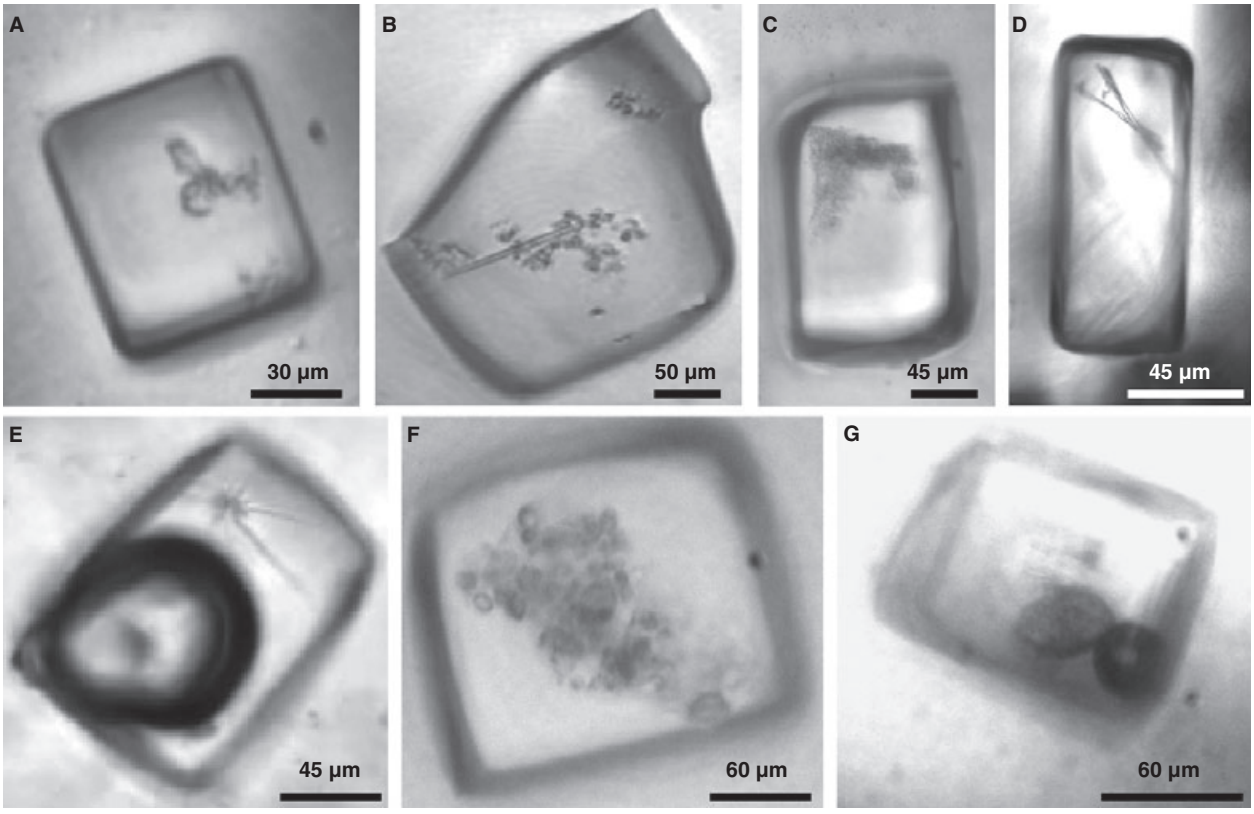

Fig. 4. Trapped solids within primary fluid inclusions in halite (A) to (F) from acid Twin Lake West. (A) Translucent to tinted red coloured hydrated sulphates, geometry of solids unrecognizable. (B) Long translucent rod shape hydrated sulphates surrounded by small tinted red coloured solids. (C) Solids are granular and red colour. (D) Translucent bladed, twined crystals. (E) Translucent and prismatic whisker crystals and vapour bubble. (F) Translucent to red coloured solid clusters. (G) Round, red coloured solid near vapour bubble from acid Lake Magic. See Fig. 5 for laser Raman spectra which shows that the solids in (A) and (B) are hydrated sulphates.

literature (Sasaki *et al.*, 1998; Frost *et al.*, 2005; Fries *et al.*, 2006; Wang *et al.*, 2006; Fleischer *et al.*, 2008). The Raman spectra of unknown natural sulphate solids contained SO_4^{2-} and H_2O peaks that matched the wavelengths of some peaks from the known hydrated sulphates. The unknown solids have other Raman peaks, especially at lower wave numbers, which did not perfectly match any of the known sulphates. A complicating factor in the identification of uncommon hydrated sulphates is that they tend to rapidly undergo dehydration, a problem not for solids within fluid inclusions, but a problem for standards measured in contact with the atmosphere (Wang *et al.*, 2006). Therefore, the majority of solids in the acid inclusions are referred to as unidentified hydrated sulphate minerals.

Fluid inclusion freezing/melting behaviours

Freezing/melting runs were performed on 49 liquid fluid inclusions from 24 halite chips from acid lakes, 18 fluid inclusions from six halite chips from synthetic acid solutions, 32 liquid fluid inclusions from 24 halite chips from neutral lakes and 14 fluid inclusions from three halite chips from synthetic neutral solutions. All fluid inclusions studied were aligned along growth bands parallel to crystal faces, had a negative crystal shape and are, in very young halite, strong evidence that they are all primary, unaltered fluid inclusions. Distinguishable differences in freezing/melting behaviour were detected between natural acid and natural neutral inclusions, between synthetic acid and synthetic neutral inclusions, and between natural and synthetic acid inclusions.

Natural acid fluid inclusions have the most complex freezing/melting behaviours (Figs 6 and 7). Acid fluid inclusions tend to have more metastable phases at specific melting temperatures than the neutral fluid inclusions, and develop a definable fuzzy border on inclusion rims. The acid fluid inclusions also generally have lower eutectic temperatures, a wider temperature range in which clear rims exist, and

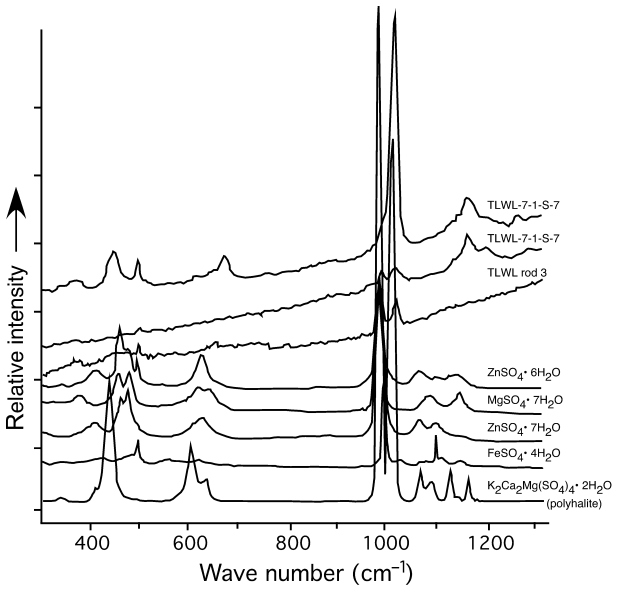

Fig. 5. Stacked Raman spectra of three solids within fluid inclusions in halite from acid Twin Lake West (top three spectra) compared with spectra from some known hydrated sulphates (bottom five spectra). Strong peaks close to 1000 cm^{-1} represent SO_4 and smaller wave numbers represent associated metals. TLWL7-1-S-7 represents hydrated sulphates from fluid inclusion A and TLWL7 represents a long translucent rod from fluid inclusion B both from Fig. 4.

more complex final melting behaviours of various crystals (Figs 6 and 7).

Only all-liquid primary fluid inclusions were used for freezing/melting analyses. However, after initial freezing and warming, a vapour bubble formed in each inclusion. Fluid inclusions froze completely between approximately −132·8 and −60·0 °C. Completely frozen inclusions were dark and opaque or, less commonly, had a clear glassy appearance. The first melting of the majority of fluid inclusions occurred between approximately −37 and −28 °C. However, natural acid fluid inclusions more commonly had eutectic temperatures between −37·0 and −33·0 °C, whereas natural neutral fluid inclusions had eutectic temperatures between approximately −36·0 and −28·0 °C (Fig. 8). The first melting was identified by the appearance of an 'orange peel' texture and the quick appearance of a vapour bubble. This early melting occurs at the centre of the fluid inclusion, whereas the inclusion wall remains dark and frozen. Upon continued warming, the dark rim dissolves and a clear rim typically forms between approximately −30·0 and −25·0 °C in natural inclusions. Clear rims appear to have high relief and are slightly birefringent under crossed-polarized light. These clear rims may be hydrohalite because of their appearance and the temperature range at which they form. Clear rims of acid fluid inclusions tend to exist for a wider temperature range (approximately −32·0 to −6·0 °C), but gradually appear as a fuzzy border upon warming from approximately −28·0 to −2·0 °C. Within neutral fluid inclusions, clear rims exist for a shorter duration and generally dissolve between approximately −20·0 and −11·0 °C. The rims in both acid and neutral fluid inclusions lighten in colour gradually as temperature increases. As the clear rim dissolves in both neutral and acid fluid inclusions, the inclusion centre darkens and becomes crowded with solids. The vapour bubble at this stage becomes irregularly shaped. This dark colour is ubiquitous within the entire volume of the acid fluid inclusion as the clear rim completely melts (refer to Fig. 6 temperatures −10·0 to −2·0 °C), whereas in neutral fluid inclusions the reaction is generally concentrated at the centre. At these same temperatures of approximately −10·0 to −2·0 °C, the fuzzy border in acid inclusions appears more distinct. This fuzzy border remains constant in acid inclusions regardless of the precipitation and dissolution of solids. The fuzzy border is interpreted as the result of a reaction between the liquid and the halite inclusion walls. The melt texture within both acid and neutral fluid inclusions becomes more blocky and the border changes to a 'building block' border as melt temperatures approach approximately −1·0 °C. This blocky border becomes most intense at approximately −1·0 °C after the majority of ice has melted and remains well above 0·0°C until unidentified solids are completely melted. The majority of remaining unidentified solids have final melting temperatures between approximately 0·0 and 2·0 °C, but also close to 3·0°C, where acid fluid inclusions commonly have final melts between approximately 2·0 and 3·0 °C.

The solids observed upon warming are very difficult to identify and quantify petrographically; they are very small (typically less than 1 μm), have a short temperature range, tend to be metastable and are crowded together. Solids appear to be metastable because they inconsistently form and dissolve within a specific temperature range. Most inclusions include hydrohalite, identified by its hexagonal shape, high relief and slight birefringence. Ice, observed as a clear rounded solid, also forms and melts well below 0·0 °C. Other solids that have been observed upon warming have cubic shapes and

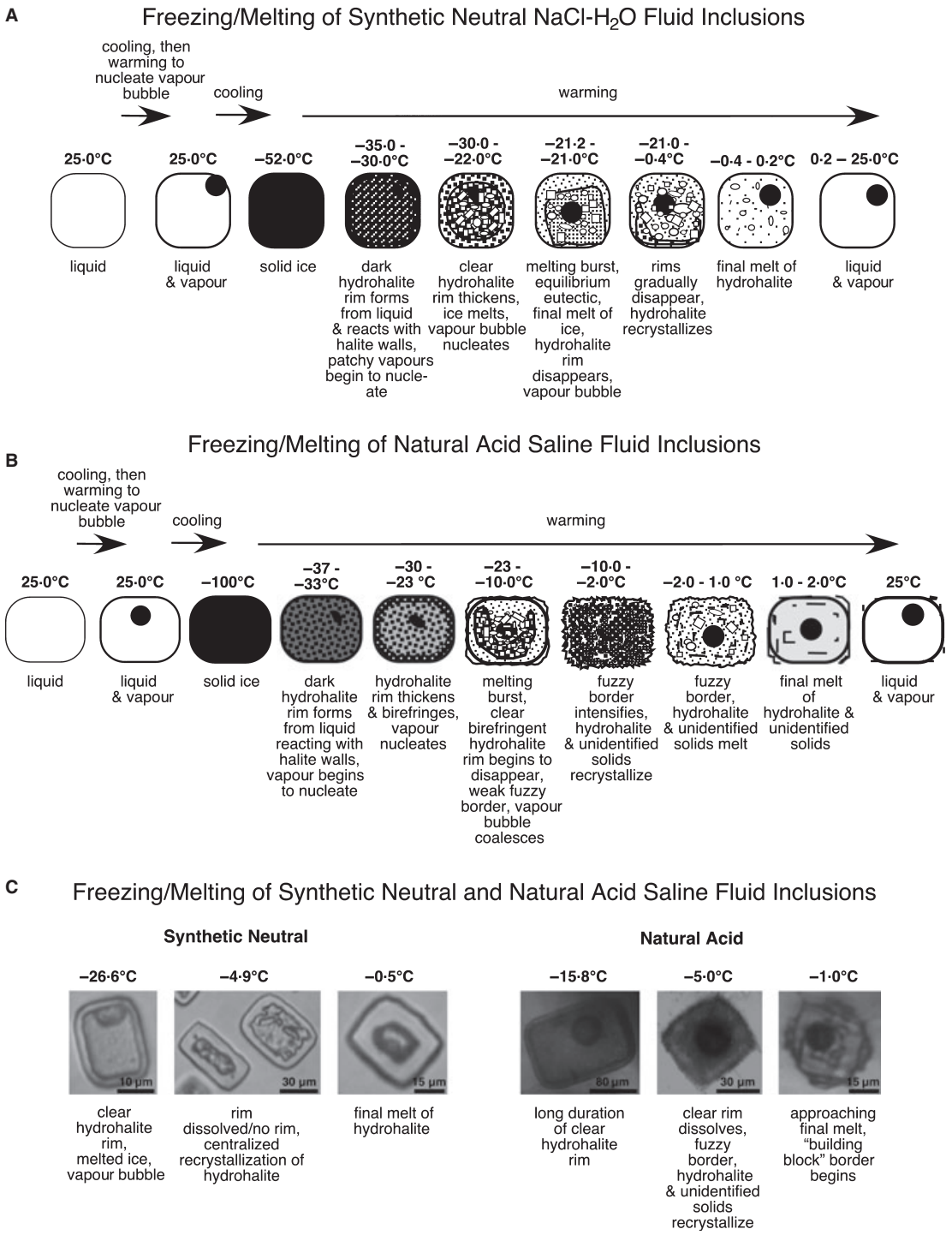

Fig. 6. Schematic diagrams of typical observations during freezing/melting runs of fluid inclusions in halite. (A) Fluid inclusion in synthetic halite grown from NaCl–H_2O solution at pH 7·0. The illustration is based upon laboratory observations, but also agrees with data in Davis *et al.*, 1990. (B) Fluid inclusion representative of natural halite from acid saline lakes in Western Australia, which contain complex Na–Cl–Mg–SO_4 solutions with some Ca and K and abundant Al, Fe, Si, Br and other elements, and have pH between 1·7 and 4·2. (C) Synthetic neutral and natural acid fluid inclusions representing phase behaviours observed at specific temperature ranges. Synthetic neutral fluid inclusions are from halite grown in NaCl–H_2O solutions at pH 7·0, except for the middle photograph fluid inclusions that were grown in NaCl–Na_2SO_4–H_2O solutions at pH 6·0. Natural acid fluid inclusions are all from Twin Lake West, pH 2·7.

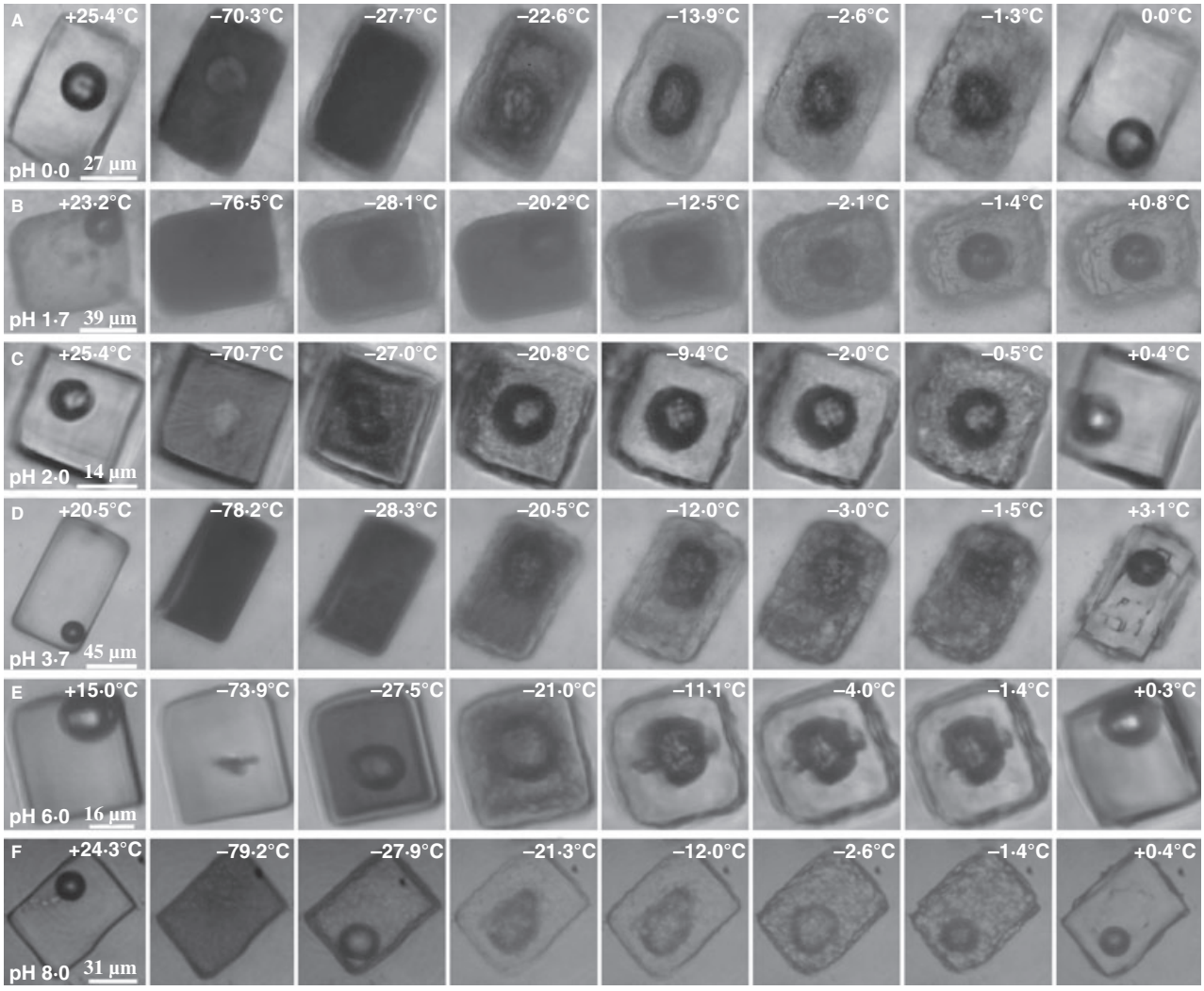

Fig. 7. Photographs of primary fluid inclusions during freezing/melting runs. Each row represents a different sample with a different pH, from most acid at the top to neutral at the bottom. Each column shows a different temperature range: room temperature is at the far left; frozen inclusions are shown in the second column from the left, with each successive column to the right showing warmer temperatures. Row A: Inclusion in synthetic halite grown from the NaCl–Na_2SO_4–H_2SO_4–H_2O system at pH 0·0. Row B: Inclusion in modern natural halite from Lake Magic (pH 1·7). Note the 'fuzzy border' between *ca* −12·5 and −2·1 °C. Row C: Inclusion in synthetic halite grown from the NaCl–Na_2SO_4–H_2SO_4–H_2O system at pH 2·0. Row D: Inclusion in modern natural halite from Twin Lake West (pH 3·7). Note the 'fuzzy border', such as shown at −12·0 °C. Row E: Inclusion in synthetic halite grown from the NaCl–Na_2SO_4–H_2O system at pH 6·0. Row F: Inclusion in modern natural halite from Lake Gastropod (pH 8·0). Note that phase behaviours in neutral inclusions (rows E and F) appear less complex when compared with acid inclusions (Rows A to D). Also note that natural acid inclusions (Rows B and D) seem to have more complex phase behaviours than synthetic acid inclusions (Rows A and C).

bladed shapes, suggesting other solids besides hydrohalite and ice.

Laser Raman analyses of liquids within fluid inclusions

Laser Raman microprobe spectroscopy (LRM) was used in an attempt to characterize any major covalently bonded compounds within the fluid inclusion liquids. All natural acid and neutral fluid inclusions analyzed with LRM showed detection of sulphate peaks at approximately 892 cm^{-1} relative wave number. All inclusion fluids also had two broad Raman peaks characteristic of water (Fig. 9). Bisulphate was not detected and has only been found in fluid inclusions with pH < 1 (Fig. 8; Benison *et al.*, 1998).

During freezing/melting runs, LRM was conducted on two acid fluid inclusions from two acid saline lakes (Lake Magic and Twin Lake West)

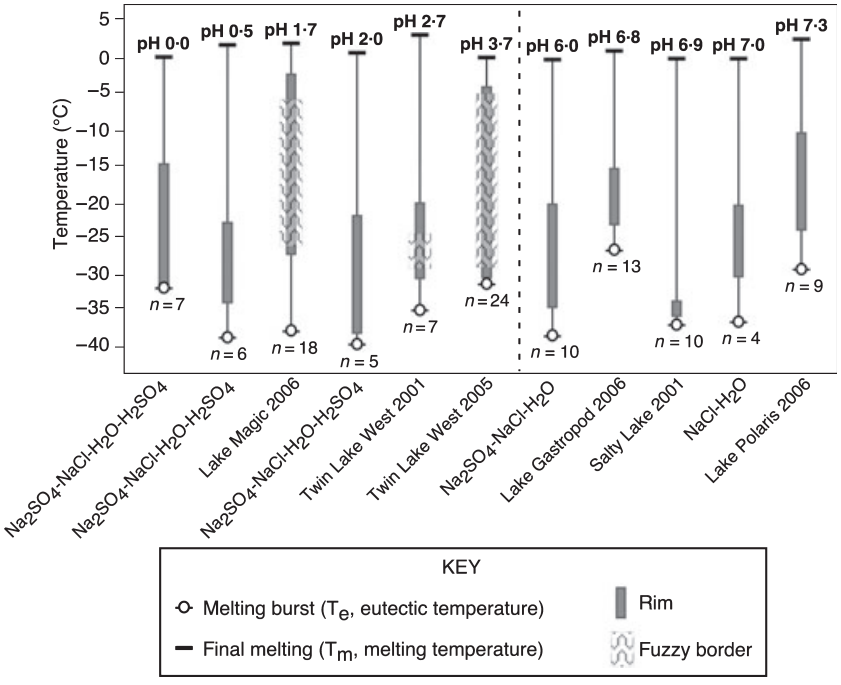

Fig. 8. Graph summarizing freezing/melting behaviours for 113 primary fluid inclusions in natural and synthetic halite. The vertical dashed line separates acid inclusion data (to the left) from neutral inclusion data (to the right). Note that 'fuzzy borders' were observed only in natural acid fluid inclusions.

and two fluid inclusions from neutral saline lakes (Gastropod West Lake and Salty Lake). The spectral results of these limited analyses show subtle differences between the acid and neutral inclusions upon temperature warming. The acid inclusions yielded small Raman peaks at approximately 400 to 550 cm^{-1} relative wavelengths, which is the same spectral range of peaks detected for the sulphate solids trapped within other fluid inclusions. A broad spectra located over the sulphate peak wavelength near 890 to 1050 cm^{-1} is present in both acid and neutral fluid inclusions. Further LRM analysis during freezing and melting needs to be done to quantify these spectral characteristics.

Biological remains in halite

Unusual biomasses, 'hairy blobs', were observed both as solid inclusions and within fluid inclusions in the acid halite, as well as within gypsum from acid lakes. Most are aligned along growth bands, closely associated with primary fluid inclusions and sulphate solid inclusions in chevron halite from acid lakes. At least 35 hairy blobs have been found in both halite and gypsum from five acid saline lakes in southern Western Australia. The pH of these lakes ranges from 2·5 to 3·0 at times when evaporites were collected. These hairy blobs, interpreted as clumps of sulphate crystals and bacterial/archaeal and fungal remains, were studied using petrography (including light microscope, SEM imaging and UV–Vis fluorescence response), SEM-EDS and laser Raman spectroscopy (fully described in Benison *et al.*, 2008).

The morphologies of hairy blobs in modern halite generally are acicular with radiating 'hairs' that extend from a central, opaque, dark body. Some appear as rounded clumps instead of acicular 'hairs' (Fig. 10); they range in size from 0·05 to 1·5 mm in diameter. Typically, the larger hairy blobs are isolated and smaller hairy blobs are found in clusters. Several primary fluid inclusions contain hairy blobs, where the interior of the inclusion is opaque and dark. Some have 'hairs' extruding outward from the fluid inclusions. The biggest inclusion observed that housed a hairy blob was 120 μm. All hairy blobs have a metallic lustre when viewed under reflected light (Fig. 10B). Polarized light microscopy shows that many hairy blobs are closely associated with micrometre-scale to millimetre-scale birefringent crystals, which Laser Raman microscopy and X-ray diffraction confirm as gypsum (Benison *et al.*, 2008).

Twelve hairy blob-filled fluid inclusions and three hairy blob solid inclusions were evaluated under multiband fluorescence and dual incidence (UV–Vis fluorescence microscopy). All three hairy blobs and some fluid inclusions strongly fluoresced under all wavelengths (365, 390, 400 and 450 nm; fig. 4 in Benison *et al.*, 2008). Various UV–Vis fluorescence excitation and emis-

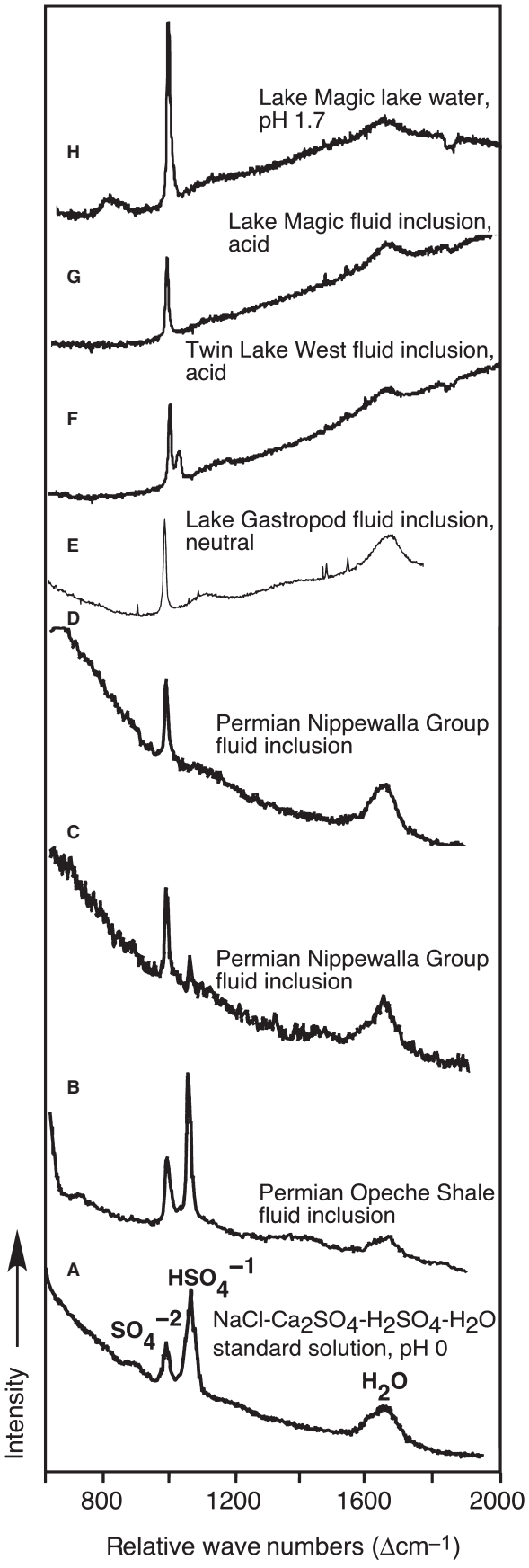

sion wavelengths suggest metabolically active biomolecules (Storrie-Lombardi *et al.*, 2001; Mormile & Storrie-Lombardie, 2005; Benison *et al.*, 2008).

Scanning electron microscopy of hairy blobs showed crystal shapes coated with and associated with biogenic-consistent textures, including bumpy surfaces on crystals, meniscus shapes between crystals, bent rods, spheres and hollow tubes (fig. 5 in Benison *et al.*, 2008). Eleven hairy blobs in halite from Twin Lake West and Prado Lake were analyzed with LRM. All hairy blobs showed broad spectral peaks, where the most common peak was 1384·1 cm^{-1} wavelength. This peak is within the range of organic carbon and disordered graphite (fig. 6 in Benison *et al.*, 2008; also, Ferrari & Roberston, 2000, 2001; Schopf *et al.*, 2002; Pasteris & Wopenka, 2003).

No 'hairy blobs' were observed in any neutral lake halites. The occurrence and characteristics of the hairy blobs strongly suggests that they are the remains of acidophilic bacteria/Archaea and fungi that lived in the acid lakes.

DISCUSSION

Similarities and differences between acid and neutral halite in Western Australia

Acid halite and neutral halite form by the same physical processes and have the same general sedimentary characteristics. In southern Western Australia, episodic flooding, evapoconcentration, desiccation and aeolian processes all strongly influence the sedimentology of the evaporites. In

Fig. 9. Stacked Raman spectra from acid saline fluids. (A) NaCl–Na_2SO_4–H_2SO_4–H_2O standard solution at pH 0·0. (B) Aqueous phase in primary fluid inclusion in bedded halite, Permian Opeche Shale, North Dakota. (C) and (D) Aqueous phase in primary fluid inclusion in bedded halite, Permian Nippewalla Group, Kansas. (E) Aqueous phase in primary fluid inclusion in bedded halite, from neutral Lake Gastropod (pH 6·8), Western Australia. (F) Aqueous phase in primary fluid inclusion in bedded halite from acid Twin Lake West (pH 2·7), Western Australia. (G) Aqueous phase in primary fluid inclusion in bedded halite from acid Lake Magic (pH 1·7), Western Australia. (H) Modern lake water, Lake Magic (pH 1·7), Western Australia. Note that all spectra contain a prominent peak for sulphate at 892 cm^{-1} and for water at 1650 cm^{-1}. Only the most acid fluids have a peak for bisulphate at 1054 cm^{-1}. Spectra of Permian inclusions modified after Benison *et al.*, 1998.

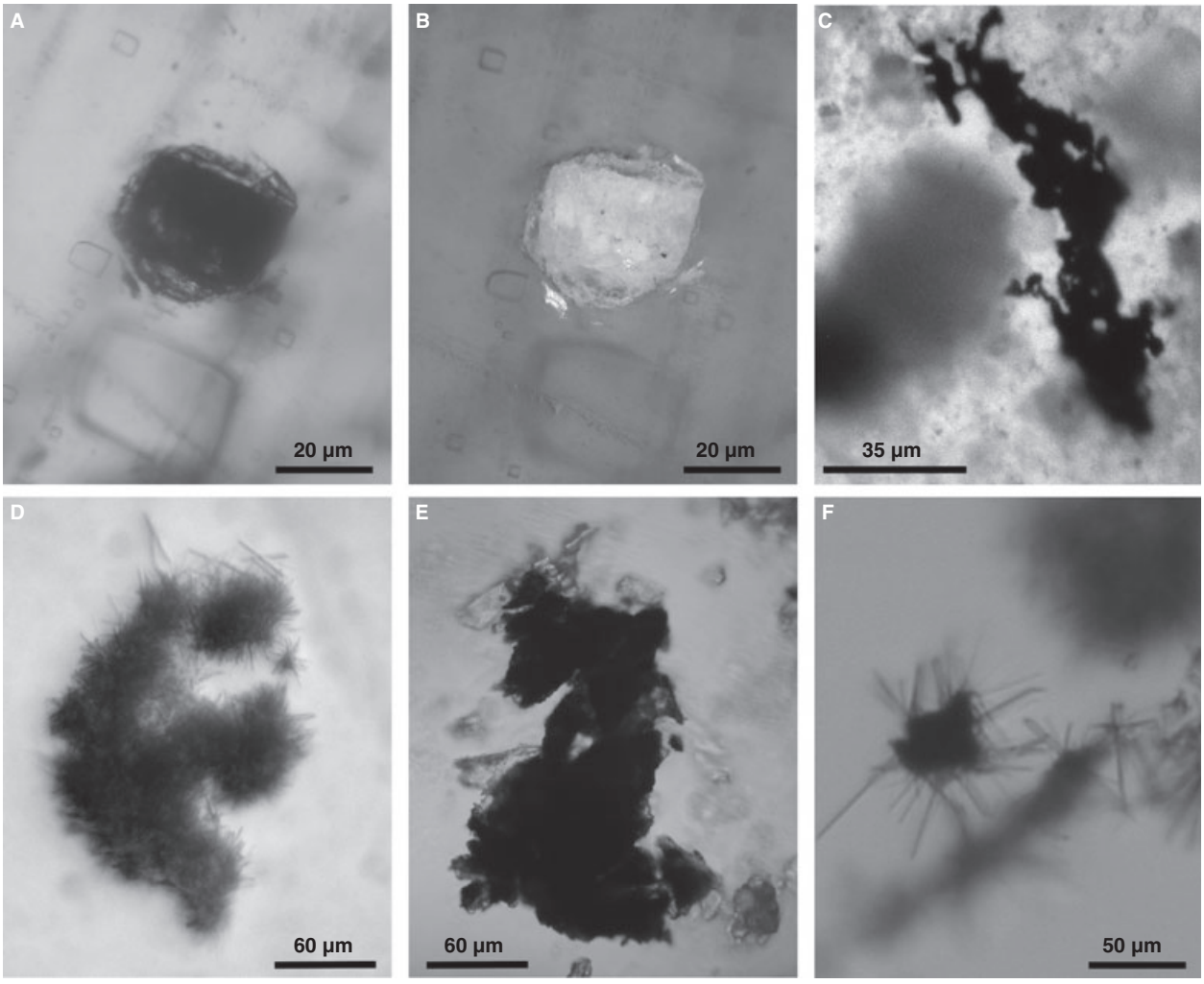

Fig. 10. 'Hairy blobs', clusters of sulphate crystals and bacterial/archaeal and/or fungal remains, in acid halite; (A) to (C) from Prado Lake, (D) to (F) from Twin Lake West. (A) and (B) show the same view of a fluid inclusion that has extruding growth of a hairy blob in transmitted plane light (A) and reflected light (B). (C) Isotropic globular hairy blob. (D) Isotropic acicular rod clusters. (E) Isotropic clusters surrounded by gypsum crystals. (F) Isotropic acicular rod cluster, possibly extruding hairy blob growth from a fluid inclusion; separate hairy blobs in background. For more phototographs and other detailed data about hairy blobs, see Benison *et al.*, 2008.

particular, flooding and evapoconcentration control the water salinity, leading to dissolution and precipitation of halite. This study focused on chevrons and cumulates, both halite crystal types that grew directly from the shallow lake waters. Both acid and neutral lakes contained chevron and cumulate halite that were sampled as they were actively growing. Both acid and neutral halites also contain growth bands defined by primary fluid inclusions.

It is important to note that both field and petrographic observations agree. That is, both the physical and chemical processes in the field that made (and at times dissolved) the halite were observed and, also, noted petrographic features within this halite reflect the field conditions. This observation is significant because it allows for a comparative sedimentological approach to be used on ancient acid and neutral halites.

There are characteristic differences between halite precipitated by acid and neutral lake waters. Acid halite commonly is coloured pale yellow or pale orange because of abundant coloured fluid or solid inclusions. Neutral lake halite is always white in the field area on the Yilgarn Craton. Acid halite, unlike neutral halite, contains abundant and diverse sulphates, both as solid inclusions and within fluid inclusions. The freezing/melting behaviours include some features such as fuzzy borders that are unique to acid inclusions. Hairy blobs occur only in the acid halite and not in the neutral halite.

These differences in acid versus neutral halite are attributed to the differences in water chemistry, specifically the pH-controlled chemical characteristics. For example, the primary acid in the lower pH waters is sulphuric acid, contributing to higher sulphur concentrations in the acid inclusions; this explains why there are more sulphate minerals in the acid systems. The acid waters have higher Fe and/or Al concentrations and, thus, precipitate hematite and make yellow water, respectively, yielding orange and yellow halite. The acid inclusions contain H_2SO_4, other sulphur species (like bisulphate) and possibly secondary acids (such as HCl and HBr), causing different reactions with the host halite during freezing/melting. Unusually high concentrations of Fe, Al, Si, Br and many metals probably contribute to the complex nature of the freezing/melting behaviours in acid inclusions. Finally, acidophilic micro-organisms would only be able to live in the acid waters, which explains their preservation only in the acid lake halite and gypsum.

Comparison of natural and synthetic halite

Using synthetic halite as standards in this study had some, but limited, value. The data from synthetic halites, when added to that of natural halites, allowed for a wide range of pH, from 0·0 to 7·3, in parent waters. This approach was particularly useful for testing the limits of bisulphate detection in fluid inclusions using laser Raman spectroscopy (Benison *et al.*, 1998), as well as exploring the range of fluid inclusion characteristics within the acid halite population.

The characteristics of freezing/melting behaviours of natural acid inclusions and synthetic acid inclusions are not distinctly comparable (Fig. 8). The synthetic fluid inclusions have consistent behaviours because of the simple parent solutions $NaCl–H_2O$, $NaCl–Na_2SO_4–H_2O$ and $NaCl–Na_2SO_4–H_2SO_4{\cdot}H_2O$. Alternately, the natural fluid inclusions, both acid and neutral, are more complex solutions, as demonstrated by the geochemical analyses of the parent lake waters (Table 2; Bowen & Benison, 2009). As a result, there is a great range in chemical compositions among acid lakes. This result leads to variations in the freezing/melting behaviours of the natural acid and neutral fluid inclusions in halite from Western Australia. Therefore, no one definitive freezing/melting profile that distinguishes acid from neutral inclusions has been found. However, there are some characteristics specific to acid fluid inclusions. Acid inclusions tend to have lower eutectic temperatures than neutral inclusions, commonly have higher final melting temperatures and have fuzzy borders.

This study shows that the complex aqueous geochemistry of natural acid systems is an important factor in determining the detailed physical and chemical characteristics of natural acid halite. This observation suggests that data from standard laboratory solutions do not necessarily give detailed insight into natural data from acid halites. For these reasons, comparisons of real data from natural acid evaporites to geochemical model results may present problems.

Comparison of modern and Permian acid halite

The Permian Nippewalla Group and Opeche Shale, which extend over much of the US midcontinent, were deposited by acid waters with extremely low pH values (< 1; Benison *et al.*, 1998). These Permian rocks are red sandstones and shales, with bedded gypsum and halite that were deposited in acid lakes and surrounding sandflats/mudflats, dunes, ephemeral channels and as palaeosols (Benison & Goldstein, 2000, 2001). These Permian rocks are lithological and chemical counterparts to the modern acid saline lake systems of southern Western Australia. Comparing the modern acid halite characteristics to the Permian acid lake halites allows testing of the criteria for the recognition of acid lake halite. In particular, it shows how these characteristics unique to acid saline systems may be preserved in the ancient rock record.

Modern and Permian halite petrography

Modern halite from acid lakes in Western Australia and Permian halite record the same types of surface and shallow subsurface processes. Both show features formed in shallow ephemeral lakes dominated by flooding–evapoconcentration–desiccation stages. Both modern and Permian acid saline lake deposits are also associated with desert soils and aeolian sands.

Permian acid halite contains abundant tiny sulphate crystals as solid inclusions and within fluid inclusions; these include gypsum, anhydrite and at least two unidentified hydrated sulphates. In addition, the Permian halite includes tiny clumps of hematite. Both Permian and modern acid lake halite are dominated by primary fluid inclusions with the same sizes, shapes and phases. Permian acid and modern acid halite are strikingly similar in their petrography.

Modern and Permian fluid inclusion chemistry

Permian lake halite fluid inclusions were analyzed for major and minor constituents, using ion chromatography and inductively coupled plasma-atomic emission spectrometry (ICP-AES; Benison & Goldstein, 2002). The inclusions contained unusually high Fe, Al and Si compared with other major elements, such as Mg and Ca. Although the modern inclusions were not analyzed in the same manner, their parent lake waters were. These waters also have unusually high Fe, Al and Si (Bowen & Benison, 2009). Both Permian and modern acid halite and their fluid inclusions have trapped sulphate solids and hematite.

Laser Raman microprobe spectroscopy determined the pH of Permian fluid inclusions. Raman spectra containing one bisulphate peak, at 1054 cm^{-1}, matched synthetic solutions with pH 0 to +1. Raman spectra with two bisulphate peaks, at 892 cm^{-1} and 1054 cm^{-1}, matched synthetic solutions with pH less than 0 (Benison *et al.*, 1998). Synthetic solutions with pH greater than +1 had no bisulphate peaks. Fluid inclusions with a sulphate peak but no bisulphate peaks can be interpreted as having pH greater than 1. Therefore, fluid inclusions with pH greater than 1 may still be acidic, but would not be identified as acidic with LRM.

The liquid phase of fluid inclusions in modern acid halite was also analyzed with LRM spectroscopy. No bisulphate peaks were noted; this agrees with pH measurements taken in the field that went as low as 1·7 pH. This observation suggests that, although detection of bisulphate peaks is a diagnostic criterion for extremely low pH, it is not a criterion for the detection of all acid waters.

The freezing/melting behaviour recognized in modern acid halite fluid inclusions, although not simple to understand, may still be an important tool for distinguishing between acid and neutral fluid inclusions. Acid fluid inclusions have lower eutectic temperatures and longer and more intensive metastable reactions that develop a fuzzy border. However, because of the complexity of both acid and neutral saline waters from Western Australia, natural fluid inclusion phase behaviours are not as consistent as those in synthetic fluid inclusions. It is important to carry out chemical analysis, such as laser Raman spectroscopy, while observing fluid inclusion freezing/melting runs.

Modern and Permian hairy blobs

Permian hairy blobs have been described in bedded chevron halite from the Opeche Shale of North Dakota (Benison & Goldstein, 2002; Benison *et al.*, 2008). The Permian hairy blobs have been found only in close association with negative pH primary fluid inclusions (Benison *et al.*, 1998). Modern hairy blobs are quite similar to Permian hairy blobs (see Benison *et al.*, 2008 for detailed descriptions and comparisons); they are similar in occurrence, general appearance, close association with sulphate minerals, and petrographic and chemical traits. However, there is greater variation in shape in modern hairy blobs in comparison with Permian hairy blobs. These biomasses have not been described elsewhere in the modern or ancient rock record. For this reason, they are considered unique to acid saline systems.

Features in Permian acid halite not observed in modern acid halite

The main differences between Permian acid halite and modern acid halite are: (i) the bisulphate peaks documented by laser Raman spectroscopy in the Permian acid halite but not in the modern acid halite; and (ii) the association with acid minerals jarosite and alunite in the modern acid halite but not the Permian acid halite. These differences may be a function of different degrees of acidity and time.

All fluid inclusions analyzed by laser Raman spectroscopy in both bedded and displacive halite from the mid Permian Opeche Shale contained at least one Raman peak for bisulphate. Some Opeche fluid inclusions contained two bisulphate peaks for bisulphate; this indicated that the Opeche Shale halite formed from lake waters and groundwaters with pH less than 1 and sometimes less than 0 (Benison *et al.*, 1998). In contrast, only 15% of the fluid inclusions in halite from the mid-Permian Nippewalla Group contained one bisulphate peak and none contained two bisulphate peaks. This observation suggests that the lowest pHs for Nippewalla waters were approximately 0 to 1, and that most of the water had pH higher than 1. Synthetic sulphuric acid solutions with pH over approximately 1 show no Raman peak for bisulphate (Benison *et al.*, 1998). No Raman peaks for bisulphate were detected in fluid inclusions from modern acid halite; this agrees with field measurements of lake pH, in which the most acidic lakes in Western Australia had pH of 1·7. This finding indicates that laser Raman spectroscopy of fluid inclusions is only a tool for confirming the most extreme pH sulphuric acid solutions.

Modern acid halite is found in the field associated with the very early diagenetic acid minerals jarosite and alunite. Mineral analyses of the Permian rocks did not detect jarosite or alunite. However, laser Raman spectroscopy of solid inclusions in Permian halite has documented at least two types of complex hydrated sulphate minerals that may be from the jarosite or alunite families. This lack of (or at least very limited occurrence of) acid minerals in the Permian rocks may be the result of a different parent water chemistry that, although both acid and Fe-rich and Al- rich, did not favour jarosite or alunite precipitation. An alternative explanation is that these relatively unstable minerals were formed in the Permian, but were weathered or altered beyond recognition over time, perhaps to become gypsum/anhydrite and hematite, both of which are abundant in these Permian rocks.

Criteria for the recognition of acid halite in the rock record

The criteria for recognizing halite that grew within acid saline waters are proposed as follows: (i) orange or yellow colour of halite because of entrapment of coloured water enriched in metals and/or entrapment of minerals common to acid waters such as hematite; (ii) abundance and diversity of sulphate minerals and/or iron oxides present as solid inclusions and within fluid inclusions in halite; (iii) freezing/melting fluid inclusion behaviours with a fuzzy border reaction rim in fluid inclusions; (iv) high Al, Fe and/or Si in fluid inclusions detected by chemical analyses (such as *in situ* analyses by environmental SEM or IC analyses of inclusion leachates); and (v) remains of microbial structures associated with accessory sulphate minerals. By considering these acid indicators when evaluating halite, especially those associated with red beds, acid saline environments in the rock record can be recognized.

CONCLUSIONS

Interpreting acid indicators within halite from modern acid saline environments has led to proposing criteria for the recognition of past acid waters in the rock record. The petrographic and chemical characteristics observed in halite from modern acid saline lakes, but absent in halite from nearby modern neutral acid lakes, may serve as such acid indicators. These acid indicators include orange or yellow colour, association with abundant sulphates and iron oxides, high Al, Fe and/or Si, fuzzy borders on fluid inclusions during freezing/melting runs, and the presence of hairy blobs. Comparison with supplemental data from synthetic acid and neutral halites and Permian acid halite helped to develop these acid halite criteria. Being able to interpret the relative pH of recent and ancient halites with these acid criteria can allow for the recognition of past extreme environments, both on Earth and on other planets.

ACKNOWLEDGEMENTS

This work is part of the undergraduate senior thesis of EAJ. Brenda Beitler Bowen, Matt Hein, Deidre LaClair, Bo-young Hong, Melanie Mormile, Franca Oboh-Ikuenobe and Stacy Story assisted in collection of halite samples in Western Australia. Brenda Beitler Bowen and Deidre LaClair conducted some fluid inclusion freezing/melting runs. Phil Oshel assisted with SEM imaging. Melanie Mormile, Jennifer Schisa and Michael Storrie-Lombardi provided help with UV fluorescence petrography. Sean Brennan, I-Ming Chou, SheRhonda Dennis and Mary Tecklenburg are acknowledged for assistance with laser Raman spectroscopy. We thank David Newell and two anonymous reviewers, Associate Editor Chris Scholz and Editor Peter Swart. Funding was provided by American Chemical Society – Petroleum Research Fund grant 35051-GB2, National Science Foundation grant EAR-0433040, and Central Michigan University.

REFERENCES

Alpers, C.N., Nordstrom, D.K. and **Spitzley, J.** (2003) Extreme acid mine drainage from a pyritic massive sulfide deposit: the Iron Mountain End-Member. In: *Environmental Aspects of Mine Waste Waters* (Eds J.L. Jambor, D.W. Blowes and A.I.M. Ritchie), *Assn. Canada Short Course Series*, **31,** 407–430. Vancouver, British Columbia.

Arthurton, R.S. (1973) Experimentally produced halite compared with Triassic layered halite-rock from Cheshire, England. *Sedimentology*, **20,** 145–160.

Benison, K.C. (2002) Can microthermometry detect sulfur compounds in fluid inclusions in halite? Preliminary results. In: *Proceedings of the Eighth Biennial Meeting of the Pan-American Current Research on Fluid Inclusions* (Eds D. Kontak and A.J. Anderson), Halifax, Nova Scotia, **8,** 7–8.

Benison, K.C. (2006) A Martian analog in Kansas: comparing Martian strata with Permian acid saline lake deposits. *Geology*, **34,** 385–388.

Benison, K.C. and **Bowen, B.B.** (2006) Acid saline lake systems give clues about past environments and the search for life on Mars. *Icarus*, **183,** 225–229.

Benison, K.C. and **Goldstein, R.H.** (1999) Permian paleoclimate data from fluid inclusions in halite. *Chem. Geol.*, **154,** 113–132.

Benison, K.C. and **Goldstein, R.H.** (2000) Sedimentology of ancient saline pans: an example from the Permian Opeche Shale, Williston Basin, North Dakota. *J. Sed. Res.*, **70,** 159–169.

Benison, K.C. and **Goldstein, R.H.** (2001) Evaporites and siliciclastics of the Permian Nippewalla Group, Kansas and Oklahoma: a case for nonmarine deposition. *Sedimentology*, **48,** 165–188.

Benison, K.C. and **Goldstein, R.H.** (2002) Recognizing acid lakes and groundwaters in the rock record. *Sed. Geol.*, **151,** 177–185.

Benison, K.C. and **LaClair, D.A.** (2003) Modern and ancient extremely acid saline deposits: terrestrial analogs for Martian environments? *Astrobiology*, **3,** 609–618.

Benison, K.C., Goldstein, R.H., Wopenka, B., Burruss, R.C. and **Pasteris, J.D.** (1998) Extremely acid Permian lakes and groundwaters in North America. *Nature,* **392,** 911–914.

Benison, K.C., Bowen, B.B., Oboh-Ikuenobe, F.E., Jagniecki, E.A., LaClair, D.A., Mormile, M.R., Story, S.L. and **Hong, B.-y.** (2007) Sedimentology of acid saline lakes in southern Western Australia: newly described processes and products of an extreme environment. *J. Sed. Res.*, **77,** 366–388.

Benison, K.C., Jagniecki, E.A., Edwards, T.B., Mormile, M.R. and **Storrie-Lombardi, M.C.** (2008) ''Hairy blobs'': microbial suspects from modern and ancient ephemeral acid saline evaporites. *Astrobiology*, **8,** 807–821.

Bobst, A.L., Lowenstein, T.K., Jordan, T.E., Godfrey, L.V., Ku, T.-L. and **Luo, S.** (2001) A 106 ka paleoclimate record from drill core of the Salar de Atacama, northern Chile. *Palaeogeogr. Palaeoclimatol. Palaeoecol.*, **172,** 21–42.

Bowen, B.B. and **Benison, K.C.** (2009) Geochemical characteristics of naturally acid and alkaline saline lakes in southern Western Australia. *Appl. Geochem.*, **24,** 268–284.

Bowen, B.B., Benison, K.C., Oboh-Ikuenobe, F.E., Story, S. and **Mormile, M.R.** (2008) Active hematite concretion formation in modern acid saline lake sediments, Lake Brown, Western Australia. *Earth Planet. Sci. Lett.*, **288,** 52–63.

Davis, D.W., Lowenstein, T.K. and **Spencer, R.J.** (1990) Melting behaviour of fluid inclusions in laboratory grown halite crystals in the systems NaCl-H_2O, NaCl-KCl-H_2O, NaCl-$MgCl_2$-H_2O, and NaCl-CaCl-H_2O. *Geochim. Cosmochim. Acta*, **54,** 591–601.

Ferrari, S.C. and **Roberston, J.** (2000) Interpretation of Raman spectra of disordered and amorphous carbon. *Phys. Rev., B*, **61,** 14095–14107.

Ferrari, S.C. and **Roberston, J.** (2001) Resonant Raman spectroscopy of disordered, amorphous, and diamond like carbon. *Phys. Rev., B*, **64,** 75414-1–75414-13.

Fleischer, I., Klingelhofer, G., Rull, F., Blumers, M., Rodionov, D., Schroder, C., Sansano, A., Medina, J., Schmanke, D. and **Maul, J.** (2008) Sulfate minerals from two Mars analogue sites Rio Tinto and Jaroso Ravine, Spain, investigated by Mossbauer and Raman spectroscopy. *Eur. Planet. Sci. Congr.*, **3,** A-00530.

Fries, M., Rost, D., Vicenzi, E. and **Steele, A.** (2006) Martian imaging analysis of jarosite in MIL 03346. *Lunar Planet. Sci. Conf.* **XXXVII,** abstract 7060.

Frost, R.L., Wills, R.-A., Weier, M.L., Martens, W. and **Kloprogge, J.T.** (2005) A Raman spectroscopic study of alunites. *J. Mol. Struct.*, **785,** 123–132.

Goldstein, R.H. (2001) Paleoenvironment: clues from fluid inclusions. *Science*, **294,** 1009–1011.

Goldstein, R.H. and **Reynolds, T.J.** (1994) *Systematics of Fluid Inclusions in Diagenetic Minerals*. SEPM Short Course 31. SEPM Society for Sedimentary Geology, Tulsa, OK.

Haynes, F.M. (1985) Determination of fluid inclusion compositions by sequential freezing. *Econ. Geol.*, **80,** 1436–1439.

Kargel, J.S. (2004) Proof for water, hints of life? *Science* **306,** 1689–1691.

Losey, A. and **Benison, K.C.** (2000) Silurian paleoclimate data through fluid inclusions in the Salina Formation halite of the Michigan Basin. *Carbonates Evaporites*, **15,** 28–36.

Lowenstein, T.K. and **Brennan, S.T.** (2001) Fluid inclusions in paleolimnological studies of chemical sediments. In: *Tracking Environmental Change Using Lake Sediments: Physical and Geochemical Methods* Vol. 2, (Eds W.M. Last and J.P. Smol), pp. 189–216. Kluwer Academic Publishers, Dordrecht, the Netherlands.

Lowenstein, T.K. and **Hardie, L.A.** (1985) Criteria for the recognition of salt-pan evaporites. *Sedimentology*, **32,** 627–634.

Lowenstein, T.K., Timofeeff, M.N., Brennan, S.T., Hardie, L.A. and **Demicco, R.V.** (2001) Oscillations in Phanerozoic seawater chemistry: evidence from fluid inclusions. *Science*, **294,** 1086–1088.

Mormile, M.R. and **Storrie-Lombardie, M.C.** (2005) The use of ultraviolet excitation of native fluorescence for identifying biomarkers in halite crystals. In: *Astrobiology and Planetary Missions* (Eds R.B. Hoover, G.V. Levin, A.Y. Rozoanov and G.R. Gladstone), Proceedings of SPIE (The International Society for Optical Engineering), Vol. **5906**, 246–253.

Mormile, M.R., Biesen, M.A., Gutierrez, M.C., Ventosa, A., Pavlovich, J.B., Onstott, T.C. and **Fredrickson, J.K.** (2003) Isolation of *Halobacterium salinarum* retrieved directly from halite brine inclusions. *Environ. Microbiol.*, **5,** 1094–1102.

Mormile, M.R., Hong, B.-y., Adams, N.T., Benison, K.C. and **Oboh-Ikuenobe, F.E.** (2007) Characterization of moderately halo-acidophilic bacterium isolated from Lake Brown, Western Australia. In: *Instruments, Methods, and Missions for Astrobiology* (Eds R.B. Hoover, G.V. Levin, A.Y. Rozanov and P.C. Davies), Proceedings of SPIE (The International Society for Optical Engineering), 66940X, 1–8

Osterloo, M., Hamilton, V.E., Bandfield, J.L., Glotch, T.D., Baldridge, A.M., Christensen, P.R., Tornabene, L.L. and **Anderson, F.S.** (2008) Chloride-bearing materials in the southern highlands of Mars. *Science*, **319,** 1651–1654.

Pasteris, J.D. and **Wopenka, B.** (2003) Necessary, but not sufficient: Raman identification of disordered carbon as a signature of ancient life. *Astrobiology*, **3,** 727–738.

Roberts, S.M. and **Spencer, R.J.** (1995) Paleotemperatures preserved in fluid inclusions in halite. *Geochim. Cosmochim. Acta*, **59,** 3929–3942.

Sasaki, K., Tanaike, O. and **Konno, H.** (1998) Distinction of jarosite-group compounds by Raman spectroscopy. *Can. Mineral.* **36,** 1225–1235.

Satterfield, C.L., Lowenstein, T.K., Vreeland, R.H. and **Rosenzweig, W.D.** (2005a) Paleobrine temperatures, chemistries, and paleoenvironments of Silurian Salina Formation F-1 salt, Michigan Basin, U.S.A., from petrography and fluid inclusions in halite. *J. Sed. Res.* **75,** 534–546.

Satterfield, C.L., Lowenstein, T.K., Vreeland, R.H., Rosenzweig, W.D. and **Powers, D.W.** (2005b) New evidence for 250 Ma age of halotolerant bacterium from a Permian salt crystal. *Geology*, **33,** 265–268.

Schopf, J.W., Kudryavtsev, A.B., Agresti, D.G., Wdowiak, T.J. and **Czaja, A.D.** (2002) Laser Raman imagery of Earth's earliest fossils. *Nature*, **416,** 73–76.

Schubert, B.A., Lowenstein, T.K. and **Timofeeff, M.N.** (2009) Microscopic identification of prokaryotes in modern and ancient halite, Saline Valley and Death Valley, California. *Astrobiology*, **9,** 467–482.

Shearman, D.J. (1970) Recent halite rock, Baja California, Mexico. *Trans. Inst. Mineral. Metall. Bull.,* **79,** 155–162.

Shearman, D.J. (1978) Halite in sabkha environments. In: *Marine Evaporites* (Eds W.E. Dean and B.C. Schreiber), SEPM Short Course, Vol. 4, 30–42.

Smoot, J.P. and **Lowenstein, T.K.** (1991) Depositional environments of non-marine evaporites. In: *Evaporites, Petroleum, and Mineral Resources* (Ed. J.L. Melvin), *Dev. Sedimentol.*, **50,** 189–347.

Squyres, S.W., Grotzinger, J.P., Arvidson, R.E., Bell, J.F. III, Calvin, W., Christensen, P.R., Clark, B.C., Crisp, J.A., Farrand, W.H., Herkenhoff, K.E., Johnson, J.R., Klingelhöfer, G., Knoll, A.H., McLennan, S.M., McSween, H.Y. Jr, Morris, R.V., Rice, J.W. Jr, Rieder, R. and **Soderblom, L.A.** (2004b) *In situ* evidence for an ancient aqueous environment at Meridian Planum, Mars. *Science*, **306,** 1709–1714.

Squyres, S.W., Arvidson, R.E., Bell, J.F. III, Brückner, J., Cabrol, N.A., Calvin, W. *et al.* (2004a) The Opportunity Rover's Athena science investigation at Meridian Planum, Mars. *Science*, **306,** 1698–1703.

Storrie-Lombardi, M.C., Hug, W.F., McDonald, G.D., Tsapin, A.I. and **Nealson, K.H.** (2001) Hollow cathode ion lasers for deep ultraviolet Raman spectroscopy and fluorescence imaging. *Rev. Sci. Ins.,* **72,** 4452–4459.

Vreeland, R.H., Rosenzweig, W.D. and **Powers, D.W.** (2000) Isolation of a 250 million-year-old halotolerant bacterium from a primary salt crystal. *Nature*, **407,** 897–900.

Wang, A., Freeman, J.J., Jolliff, B.L. and **Chou, I.-M.** (2006) Sulfates on Mars: a systematic Raman spectroscopic study of hydration states of magnesium sulfates. *Geochim. Cosmochim. Acta*, **70,** 6118–6135.

Manuscript received 24 July 2009; revision accepted 4 September 2009